Impact of regional-scale atmospheric circulation patterns on winter air temperature variability in the Svalbard area

Ewa BEDNORZ* ORCID- 0000-0002-5156-5568, Arkadiusz M. TOMCZYK ORCID-0000-0003-1576-8795, Bartosz CZERNECKI ORCID-0000-0001-6496-1386 and Miłosz PIĘKNY

Department of Meteorology and Climatology, Institute of Physical Geography and Environmental Planning, Adam Mickiewicz University, B. Krygowskiego 10, 61–680 Poznań, Poland
* *corresponding author <ewabedno@amu.edu.pl>*

Running title: Regional-scale circulation patterns in the Svalbard area

Abstract: Significant increasing trends in the air temperature were found both in the surface station of Svalbard Lufthavn and in the low-tropospheric temperature field over the Atlantic Arctic. The variability in temperature, as well as the multiannual trend, is at least three times bigger in the winter months than in summer. An attempt was made to explain the high day-to-day variability in the winter air temperature by the daily variability in the regional pressure field and circulation conditions. Six regional-scale circulation patterns were found by applying the principal component analysis to the mean daily sea level pressure (SLP) reanalysis data and their impact on the low-tropospheric air temperature variability was determined. A bipolar pattern, with a positive center over Greenland and a negative center over the White Sea, dominates in the region and strongly influences the air temperature field at 850 hPa geopotential height (correlation coefficients up to –0.65). The second pattern that impacts the temperature field in the Atlantic Arctic is the one with a center of action over Svalbard (mostly a low-pressure center in winter), strongly influencing the air temperature over the Barents Sea. The remaining circulation types, explaining only 5–8% of the total variance of the SLP field each, do not modify significantly the air temperature at 850 hPa geopotential level over the Atlantic Arctic, and none of the circulation types seems to influence the multiannual temperature trends.

Keywords: Arctic, Spitsbergen, weather patterns, sea level air pressure, temperature trends.

Introduction

Modern warming is most intensely manifested in the Arctic and displays an intensive increase in air temperature, which remains three times higher than the global average, and also record-high air temperatures over recent years (AMAP 2021). For example, in 2020 record high air temperature of 21.7°C was observed in Longyearbyen (Spitsbergen) (Severe Weather Europe 2020), and in Verkhoyansk (Siberia), air temperature exceeded 30°C for approximately a dozen days, with a maximum on 21 June, reaching 38.0°C (WMO 2020). The increasing frequency of positive temperature extremes occurrence in the Arctic, both in summer and winter, was documented in several studies (Tomczyk and Bednorz 2014; Matthes *et al.* 2015; Vikhamar-Schuler *et al.* 2016; Wei *et al.* 2016; Tomczyk *et al.* 2019). These changes are accompanied by a decreasing number of negative extremes (Niedźwiedź *et al.* 2012; Łupikasza and Niedźwiedź 2013; Tomczyk 2014; Tomczyk *et al.* 2019). Matthes *et al.* (2015) documented a positive trend in the occurrence of warm spells and a strong decreasing trend in the occurrence of cold spells in the Arctic both in winter and summer. The greatest increase in mean air temperature, computed for the period 1971–2019, was observed in the cold season (Oct–May) over the Arctic Ocean (4.6°C on average), and the maximum warming (by 10.6°C) proceeded over the northeastern Barents Sea (AMAP 2021). The warming process accelerates and in the Atlantic Arctic, the warming pace for the mean annual temperature increased from 0.35°C per decade in the period 1951–2015 to 1.40°C per decade in the recent decades 1996–2015, and even more for the winter months – from 0.46°C per decade to 2.59°C per decade (Przybylak and Wyszyński 2020).

The primary cause of the Arctic warming in the late 20th and beginning of the 21st century is anthropogenic greenhouse gas emissions into the atmosphere, however, several feedback effects and other interactions intensify the process in this region (Johannessen *et al.* 2004; Serreze and Francis 2006; Fyfe *et al.* 2013). One of them is the reduction in sea ice extent, related to the additional heat release to the atmosphere, as well as water vapour content (Overland and Wang 2010; Overland *et al.* 2011; Park *et al.* 2015; Alekseev *et al.* 2016). These mechanisms lead to more intensive and rapid warming in the Arctic than anywhere else on the Earth, which is referred to as Arctic amplification (Serreze and Francis 2006). Different processes, apart from anthropogenic greenhouse gas emissions, have been recognized as reasons for the early 20th century Arctic warming, recorded in the first half of the century and reaching a peak in the years 1920–1940. For example, the anomalous atmospheric circulation over the sectors of the North Pacific and North Atlantic forced by sea surface temperature, particularly in the North Atlantic, played an important role in the early 20th century Arctic warming episode (Bengtsson *et al.* 2004;

Nozawa *et al.* 2005; Polyakov *et al.* 2010; Tokinaga *et al.* 2017; Łupikasza and Niedźwiedź 2019; Łupikasza *et. al* 2021). Przybylak *et al.* (2022) claim, that changes in atmospheric circulation forced the early 20th century warming in 71.6%, and oceanic circulation in 20.6%. Łupikasza and Niedźwiedź (2019) evidenced that on Spitsbergen the period of the early 20th century was characterised by a considerably greater frequency of warm southern circulation patterns, and a lower frequency of cold northern circulation patterns.

Undoubtedly, atmospheric circulation is one of the most important factors affecting weather and climate conditions, and its changes significantly determine short- and long-term variability of weather conditions, including air temperature (Yarnal 1993). This is particularly true for high latitudes in winter – without solar radiation. Several circulation patterns modifying the weather variability in the Arctic were identified in the monthly time scale. The first, known as Arctic Oscillation (AO), was first recognized and named by Thompson and Wallace (1998), and Deser (2000) as the leading Empirical Orthogonal Function (EOF) of monthly SLP anomalies in winter poleward of 20°N. Skeie (2000) and Chen *et al.* (2013) found Barents Oscillation as the second EOF of monthly SLP anomalies poleward of 30°N. Both teleconnection patterns are most evident in the winter months and Arctic Oscillation was proven to have a strong impact on the Northern Hemisphere temperature field (Thompson and Wallace 1998; Wang *et al.* 2005). Cai *et al.* (2018) reproduced the Arctic Dipole (a Barents Oscillation variant), as the second after AO circulation pattern during the Arctic summer, neither as strong in terms of the variance explained nor as stable as the AO. The Greenland Blocking Index, which represents and depicts changes in blocking across the entire Greenland region, has been defined by Fang (2004) and popularized by Hanna *et al.* (2016).

The basic aim of the study is to recognize circulation patterns that occur on a daily time scale, explain the changeability in the SLP field in the Atlantic Arctic region, centered at Svalbard Archipelago, and find out their influence on short-term variability in the low-tropospheric temperature field in the region, as well as on the surface temperature in Spitsbergen island, represented by Svalbard Lufthavn station. Furthermore, the multiannual trends in the recognized circulation patterns' phases and intensity could provide additional factors for explaining the winter warming intensity in the Atlantic Arctic.

Study area

The area of the study covers the Atlantic part of the Arctic and the Northern Atlantic Ocean with the encompassing lands of Greenland, Iceland, and northern Europe (Fig. 1). The

research is focused on the Svalbard Lufthavn station (78.25°N, 15.46°E, 2 m a.s.l.) located on Spitsbergen island belonging to Svalbard Archipelago. The station is situated at the inner end of Adventfjorden, a southern branch of Istfjorden, which is cut deeply into the land from the west side and opened to the western and southwestern air flows (Nordli 1990).

The archipelago is located in the middle of the study area, bordered by the Arctic Ocean in the south, the Barents Sea in the southeast, and it is detached from Greenland by the wide Fram Strait in the southwest. The Atlantic region is characterized by the highest temperatures in the entire Arctic during the cold season, due to intense cyclonic activity and branches of the warm North Atlantic current reaching the far north. The same factors cause the highest variability in meteorological elements in the region, particularly the air temperature (Przybylak 2016).
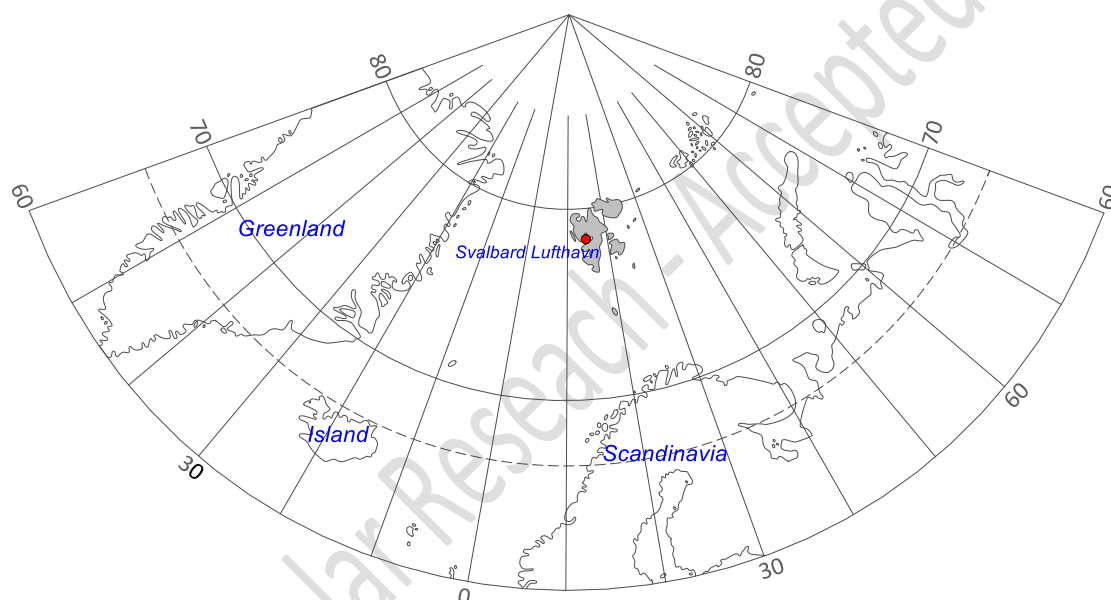

Fig 1. Study area with Svalbard Archipelago marked in grey; location of Svalbard Lufthavn station marked with a red dot.

Methods

Daily mean air temperature data for the Svalbard Lufthavn station (Fig. 1) for the years 1976–2021 were collected from the Norwegian Meteorological Institute dataset (available at https://seklima.met.no/. Only the four coldest months (December–March, then referred to throughout the text as winter) were taken to the main analysis, however, some basic calculations were provided also for the warmest months (June–August), to show the difference between the seasons. Additionally, NCEP/NCAR (National Centers for Environmental Prediction/National Center for Atmospheric Research) reanalysis data, concerning daily mean air temperature at 850

hPa geopotential level in the years 1976–2021 were obtained from the NOAA ESRL PSD (National Oceanic and Atmosphere Administration, Earth System Laboratory, Physical Sciences Division) resources (Kalnay *et al.* 1996). To identify circulation patterns, SLP reanalysis data were derived from the same source. NCEP/NCAR reanalysis data have 2.5°×2.5° resolution, which was reduced along parallels to 5° for latitudes 60–70°N and to 10° for latitudes 72.5–87.5°N, to obtain more even grid distribution along parallels and meridians.

The obtained data provided the basis for the calculation of mean annual and mean monthly air temperature, as well as mean air temperature in the winter season (December–March). Next, the direction and rate of changes were computed and the significance of the rate of change was verified using a t-Student test. Based on the calculated mean values, the lowest and highest mean value in the analysed multiannual period was determined for each month. Moreover, 10 coldest and warmest winter seasons were identified.

Cold days were then designated, defined as days with mean daily air temperature lower than temperature corresponding with 10. percentile of daily temperature. Warm days were identified as days with mean daily air temperature exceeding 90. percentile from daily air temperature. Threshold values corresponding with 10. and 90. percentiles were calculated for each decade of the winter season. The occurrence of the identified days was then analysed, and the direction and rate of changes in their occurrence were determined. The statistical significance of trends was assessed by means of a non-parametric Mann-Kendall test, adopting $\alpha \leq 0.05$ for significant trends. The trend in the analysed characteristics was determined by means of the related Sen's slope method (Mann 1945; Kendall 1975; Salmi *et al.* 2002).

To develop the daily regional circulation patterns the principal component analysis with varimax rotation (PCA) was applied to standardized SLP daily data (Huth 1996; Huth *et al.* 2008; Wilks 2011; Huth and Beranová 2021). Standardization allowed to deseasonalize the observations, keeping the intensity of daily SLP fields in the analysis, and maintaining the daily temporal scale of the original data (Esteban *et al.* 2005). The PCA is a multivariate statistical technique that reduces a large number of variables in a data set and it is widely used in the atmospheric sciences to accomplish types of circulation patterns (Barnston and Livezey 1987; NCAR 2015). In this study, the daily SLP values acted as the observations, and the grid points made up the variables, which number was reduced to fewer new variables – namely principal components (PCs). PCs stand for circulation types, and they express the variability of the SLP field, having the percentage of explained SLP variance specified for each of them. Each of the obtained PC has a new daily time series of eigenvalues, which are used as daily indices of a

particular circulation type, showing its strength and positive or negative sign. Furthermore, loadings of each PC, which show the spatial pattern of correlation between the old variables (standardized gridded daily SLP values in this case) and the new ones (daily indices of each PC), are obtained in the analysis (Wilks 2011). Six PCs were chosen for analysis in this study, using the criterion that a minimal percentage (75%) of the total variability of the raw data must be represented by the chosen principal components.

Relationships between air temperature and circulation patterns were established by Pearson's correlation coefficient, and the statistical significance of the correlation indices was tested using Student's t–distribution for probability level p = 0.05.

Results

Air temperature variability and trends. — In the period 1976–2021, mean annual air temperature in Svalbard Lufthavn station was –4.7°C. The lowest mean value was recorded in 1988 (–8.9°C), and the highest in 2016 (–0.2°C). The analysis showed an increase in mean annual air temperature that was statistically significant and reached 1.14°C per decade. High variability of thermal conditions was observed in the analysed station. Mean annual air temperature amplitude was 19.6°C. On average, the lowest mean monthly air temperature was recorded in March, when it reached –12.9°C (Fig. 2). Approximate values were observed in February and January, namely –12.7°C and –12.2°C, respectively. In December, mean air temperature was higher, reaching –10.4°C. The above data show that the coldest period in station Svalbard Lufthavn was from December to March, with an average below –10.0°C each month. The highest mean monthly air temperature was recorded in July at a level of 6.7°C. Except for the warmest month, the value of mean monthly air temperature exceeded the threshold of 0°C only in three other months, *i.e.*, in August (5.6°C), June (3.1°C), and September (1.5°C). In the analysed multiannual period, the lowest mean air temperature for each month was recorded in the 20th century, particularly in the 1970s and 1980s (Table 1). The highest mean monthly value was observed in years from the 21st century, except for September (1990) and December (1984). The lowest mean monthly air temperature was recorded in March 1977 (–23.3°C), and the highest in July 2020 (9.8°C). In the study period, an increase in mean monthly air temperature was observed in all months, and the most intensive changes occurred in winter months with a maximum in January (2.23°C per decade).
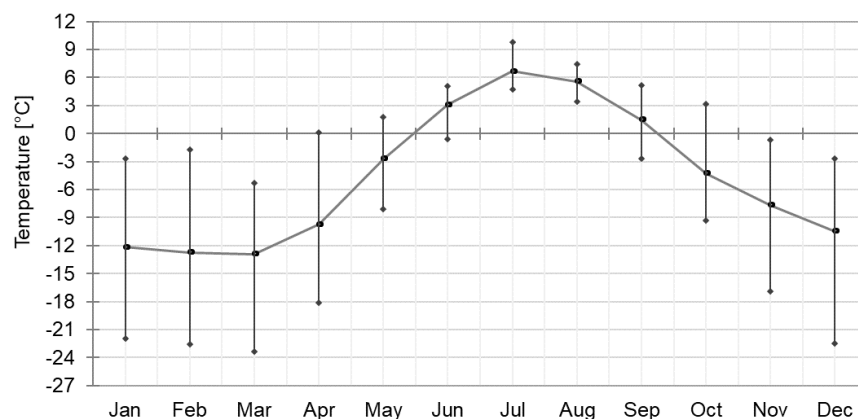
Fig. 2. Annual course of monthly mean annual air temperature with maximum and minimum mean monthly values in the period 1976–2021 in Svalbard Lufthavn station.

Table 1.

Characteristics of monthly air temperature in Svalbard Lufthavn station: mean, maximum and minimum with a year of occurrence and trend.

Month	Warmest month		Coldest month		Average temperature (°C)	Changes (°C per decade)
	Temperature (°C)	Year	Temperature (°C)	Year		
Jan	−2.7	2006	−22.0	1981	−12.2	2.23
Feb	−1.7	2014	−22.5	1986	−12.7	2.04
Mar	−5.3	2012	−23.3	1977	−12.9	0.89
Apr	0.1	2006	−18.1	1988	−9.7	1.26
May	1.8	2018	−8.1	1979	−2.7	0.84
Jun	5.1	2007	−0.6	1979	3.1	0.67
Jul	9.8	2020	4.7	1987	6.7	0.49
Aug	7.5	2002	3.4	1994	5.6	0.51
Sep	5.2	1990	−2.6	1982	1.5	0.85
Oct	3.2	2016	−9.3	1988	−4.3	0.88
Nov	−0.7	2016	−16.9	1988	−7.7	1.28
Dec	−2.7	1984	−22.5	1988	−10.4	1.74

In the analysed multiannual period, mean air temperature in winter was –12.1°C, in particular seasons varying from –18.7°C (1988/89) to –5.2°C (2011/12). In most seasons until the beginning of the 21st century, mean air temperature was maintained below the average from the multiannual period, and during the coldest season the anomalies reached –6.7°C. In the 21st century, most seasons were characterised by mean air temperature above the average from the

multiannual period, and in the warmest season, the anomalies reached 6.9°C. Among the ten coldest winter seasons, nine were recorded in years from the 20th century, and in the case of the warmest seasons, nine occurred in years from the 21st century (Table 2). The study revealed a statistically significant increase in mean air temperature at a level of 1.83°C per decade (Fig. 3).
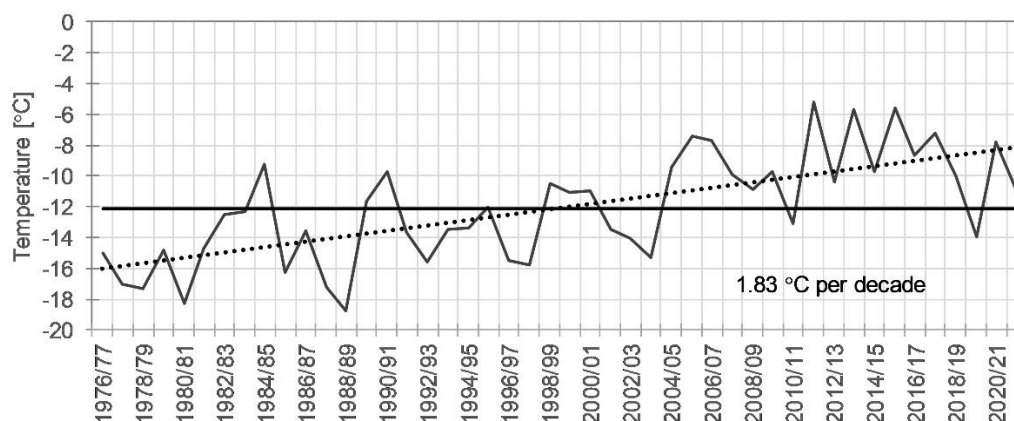

Fig. 3. Multiannual course of mean winter (Dec–Mar) air temperature (°C) in Svalbard Lufthavn station with the trend of changes, trend line (dotted) and the mean value from 1976/77–2020/21 marked with a horizontal line.

Table 2.

The warmest and the coldest winters (Dec–Mar) in Svalbard Lufthavn station.

	Warmest		Coldest	
	Year	Mean temperature (°C)	Year	Mean temperature (°C)
1	2011/12	–5.2	1988/89	–18.7
2	2015/16	–5.5	1980/81	–18.3
3	2013/14	–5.7	1987/98	–17.2
4	2017/18	–7.2	1978/79	–17.2
5	2005/06	–7.3	1977/78	–17.0
6	2006/07	–7.7	1985/86	–16.3
7	2020/21	–7.8	1997/98	–15.7
8	2016/17	–8.7	1992/93	–15.4
9	1984/85	–9.1	1996/97	–15.4
10	2004/05	–9.5	2003/04	–15.3

Based on the adopted definition, 6 warm and cold days were recorded on average in a season. The highest number of warm days was observed in winter 2005/06, *i.e.*, as many as 20 days (Fig. 4). Equally many (>15 days) warm days occurred in seasons 2011/12, 2013/14, and 2015/16. In the study period, no warm days were recorded during three winters, including 1980/81, 1988/89, and 2019/20. The study period showed a statistically significant increase in the frequency of warm days at a rate of 1.27 days per decade.

High variability of occurrence of cold days was determined in the study period. The highest number of such days was recorded at the beginning of the studied multiannual period with a maximum in season 1988/89 (25 days) (Fig. 4). Equally numerous cold days occurred in winter 1980/81 (22 days) and 1977/78 (20 days). An evident decrease in the frequency of cold days occurred in the 21st century, and during the last decade they were only recorded in winter 2019/20 (3 days). A decrease in the number of cold days was recorded at a level of 2.95 days per decade, and the changes were statistically significant.
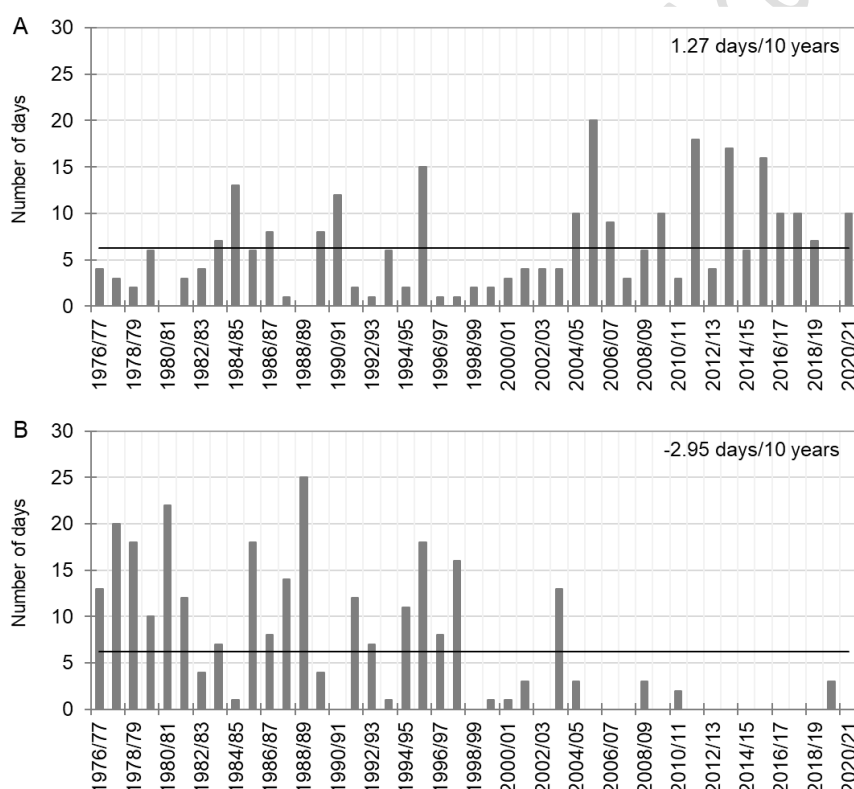

Fig. 4. Number of warm (A, mean temperature >95 percentile) and cold (B, mean temperature <5 percentile) days in winter (Dec−Mar) in Svalbard Lufthavn station with the trend of changes and a mean value indicated by a horizontal line.

A significant increase in low-troposphere air temperature in winter was observed not only in the Svalbard region, as specified by the example of the Svalbard Lufthavn station, but over almost the entire Atlantic Arctic. The rate of changes, computed for the air temperature reanalysis data, exceeded 0.3°C per decade in the period 1976–2021 (Fig. 5). The area of the most intense low-tropospheric warming with an increase rate of >0.7°C per decade encompasses the Svalbard Archipelago and the area east to Svalbard, including the northern part of the Barents Sea, Franz Josef Land, and northern Novaya Zemlya. In the western part of the study area represented by Greenland, the slowest warming was observed in the south (<0.3°C per decade), which was intensifying to the north, where the temperature-increase rate exceeded 0.6°C per decade (Fig. 5, DJFM). The warmest months (Jun–Aug) were characterized by a much slower pace of change in low tropospheric temperatures and the trends varied from zero over central Greenland to more than 0.4 °C per decade over the Fram Strait, northern Scandinavia, and Baffin Sea (Fig. 5,JJA).
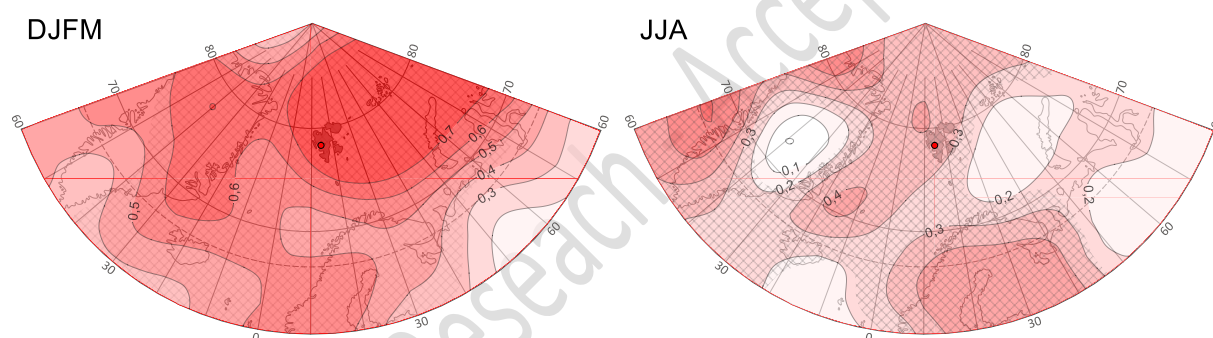

Fig. 5. Changes in reanalysis air temperature at 850 hPa geopotential level (°C per decade) in winter (DJFM, Dec–Mar, left) and in summer (JJA, Jun−Aug, right) in the period 1976–2021. Areas of statistically significant trends (p >0.05) are checked; Svalbard Archipelago is shaded grey; Svalbard Lufthavn station is marked with a red dot.

Impact of regional-scale SLP patterns on Svalbard air temperature. — In the Arctic, more than anywhere else on the Earth, the air circulation, *i.e.*, advection of the particular air masses triggered by the pressure patterns, influences the air temperature. To establish the basic relationship between the surface temperature in the Svalbard region and the pressure field in the Atlantic Arctic, the correlation coefficients between the anomalies of daily mean surface air temperature in the Svalbard Lufthavn station and the grid-points SLP values were computed for winter months (Dec–Mar) and (for comparison) for summer (Jun–Aug) (Fig. 6). In winter a bipolar correlation field appeared, with the negative and positive correlation centers extending

zonally at approximately 70–80°N. The negative center (–0.4) is located west of the Svalbard Archipelago in the region of the northeastern Greenland coast. The value of correlation below –0.3 encompassed the area along the eastern coast of Greenland, including Fram Strait and the west Greenland Sea. The opposite center with a correlation coefficient exceeding 0.4 extended over the northern Eurasia coast from the White Sea to the Yamal Peninsula, including the surrounding Arctic waters. Such a correlation field means that higher/lower than normal pressure in the east/west increases the air temperature in Spitsbergen, simply by enhancing southern air flow, while the opposite SLP pattern intensifies the northern flow, which brings cold air to Svalbard Archipelago. The location of the Svalbard Lufthavn station at the fiord deeply cut inland from the west side of Spitsbergen island and oriented SW−NE, makes the air temperature at the station particularly vulnerable to the airflow along the fiord, enhanced by the pressure patterns imitated in Fig. 6 (DJFM). A much lower correlation was detected in the summer months (Jan–Aug) and the only area, where the coefficient exceeded 0.3 appeared northeast of Spitsbergen in the Franz Josef Land area.
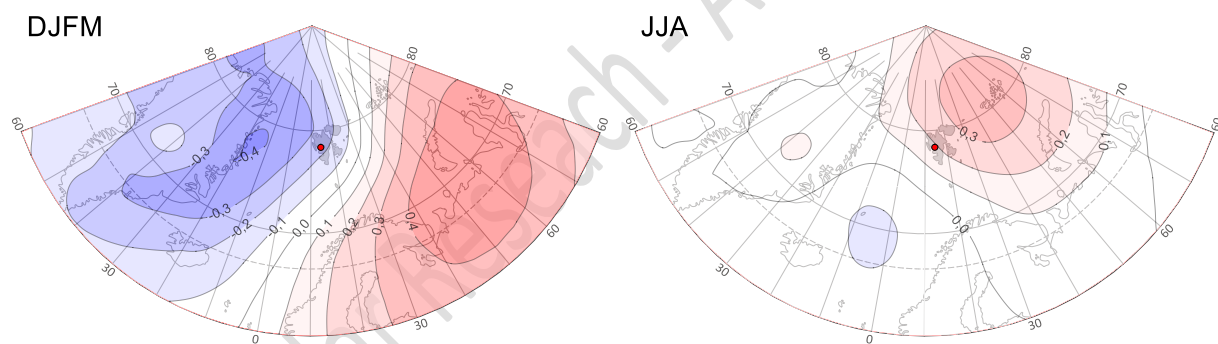

Fig. 6. Correlation between daily air temperature anomalies in Svalbard Lufthavn station and sea level pressure in winter (DJFM, left) and in summer (JJA, right) for winters 1976/77–2020/21. Svalbard Archipelago is shaded grey; Svalbard Lufthavn station is marked with a red dot.

The regional-scale circulation patterns in the Atlantic Arctic were developed by applying PCA to the standardized SLP daily data matrix. Six PCs, representing together 76% of the total SLP field variance, were selected (Table 3). In Fig. 7, the percentage of SLP variance explained by each of chosen six PCs, as well as their loadings, i.e. spatial patterns of correlation between the daily standardized SLP values and daily indices time series of each PC, are displayed.

Positive/negative correlation indicates areas of the higher/lower than normal SLP in the positive phase of a given circulation type (PC1–PC6).

The first PC explains most of the total SLP variability within the study area (26.9%) and it discloses a bipolar pattern, with a positive center over Greenland and a negative center over the White Sea. In the positive phase of PC1, the Greenland High strengthens, while lower-than-normal pressure, possibly forming a local cyclone in a strong positive PC1 phase, appears southeast of Svalbard. Such a pressure pattern induces a northeastern inflow of cold air masses over the archipelago, whereas the negative phase, denoting the opposite SLP pattern, brings about warm air from the southwest (Fig. 7). During winter, no positive or negative phase of the PC1 prevails on average, since April the positive phase is more often, until summer months when an average index value is negative (Fig. 8).

The next circulation pattern PC2 is less important than PC1, as it represents 16.2% of the total SLP variance. Similarly to PC1, PC2 is also characterized by a bipolar pattern of loadings, although quite differently oriented. In a positive phase of PC2 stronger-than-normal cyclonic activity (a negative sign of loadings) is observed over the Norwegian Sea, and a high-pressure area extends in the east and northeast of the studied area, with the highest positive values of loadings over the Franz Josef Land (Fig. 7). Thus, in the positive/negative phase of PC2 southeastern/northwestern airflow prevails over Spitsbergen. The annual average course of PC2 indices shows a positive phase with southeastern flow dominating in winter and a negative phase prevailing in summer (Fig. 8).

Under the positive phase of PC3 (explaining 13.4% of total SLP variance) an anticyclonic center forms right over Svalbard Archipelago, while lower-than-normal pressure is observed in the west and the southeast (Fig. 7). Cyclonic conditions accompanied by negative PC3 indices are predominant in the cold season, while positive indices prevail in summer (Fig. 8). Each of the three remaining PCs explains less than 10% of the total variance of the SLP field and they display patterns with several secondary centers of action.
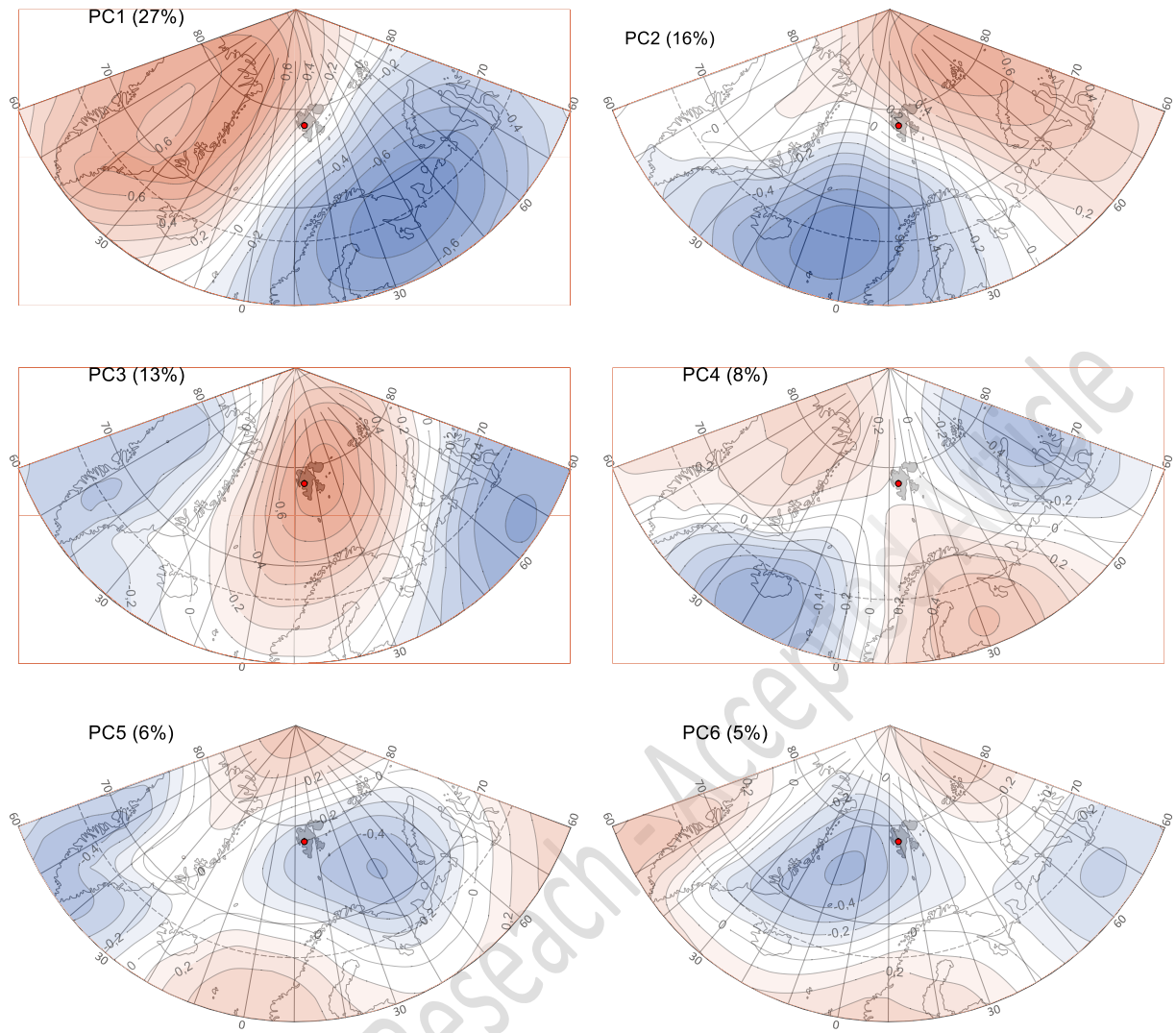
Fig. 7. Regional circulation patterns in the Svalbard area – spatial patterns of correlation between the standardized daily SLP values and the daily indices of each PC (based on 1976–2021 SLP data). Svalbard Archipelago is shaded grey; Svalbard Lufthavn station is marked with a red dot.
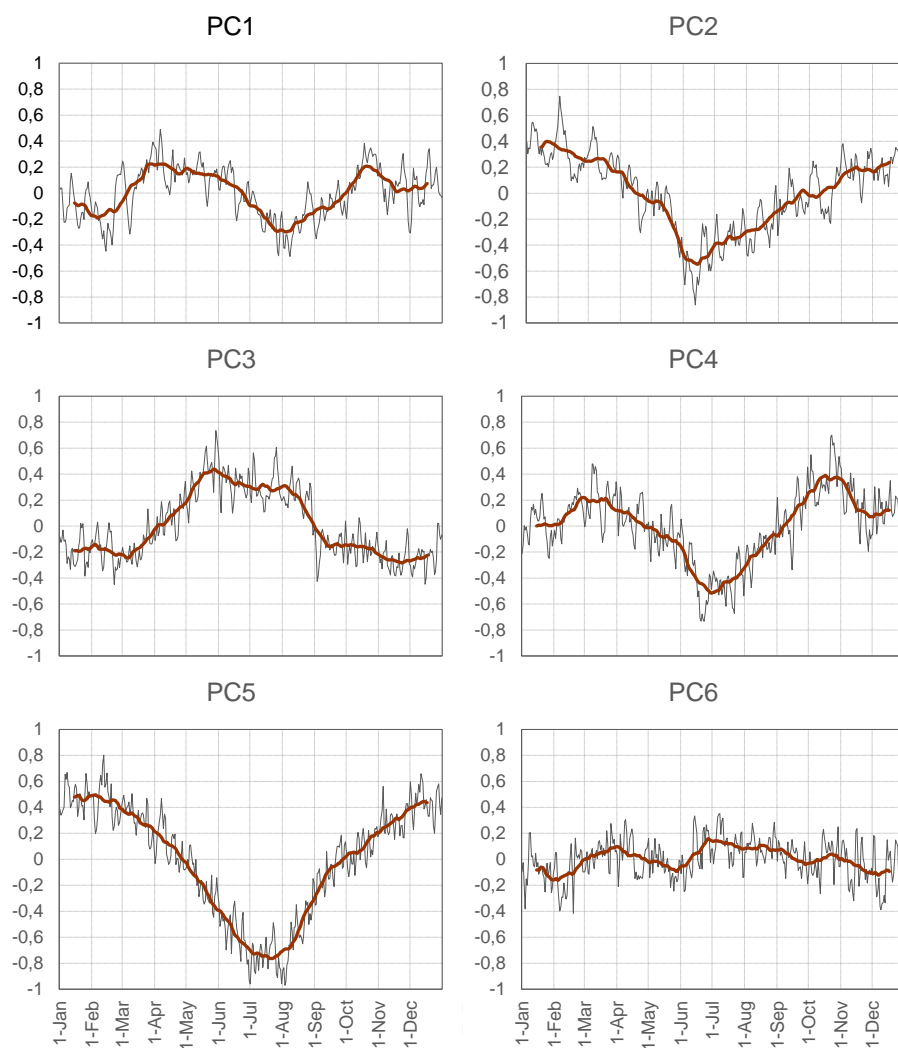
Fig. 8. Annual daily course of circulation pattern indices averaged for the period 1976–2021 with the 30-day moving average.

Table 3.

Results of PCA, including the percentages of the total variance of the SLP field, explained by the first six principal components (PCs), and the correlation coefficient (*r*) between each PC's daily indices and the daily mean air temperature anomalies in Svalbard Lufthavn station from December to March. Value statistically significant at p >0.05 is marked in bold.

	Total variance (%)	Cumulated total variance (%)	*r*
PC1	26.9	26.9	**−0.55**
PC2	16.2	43.1	0.16
PC3	13.4	56.5	−0.13
PC4	8.0	64.4	−0.11

| PC5 | 6.5 | 70.9 | −0.11 |
| PC6 | 5.4 | 76.3 | 0.19 |

In the next step, it was determined, how each of the developed circulation patterns modifies the air temperature field in winter. The correlation coefficient (r) between the time series of each PC daily indices and the daily mean air temperature anomalies at 850 hPa geopotential height from December to March was computed and mapped (Fig. 9). PC1 which is the dominant pattern in the Atlantic Arctic, reveals the strongest impact on the winter air temperature of all the developed circulation types. The negative relationship occurs over most of the studied area, being strongest ($r<–0.6$) between Iceland and Svalbard. In the positive phase of PC1, the weather in this area is influenced by enhanced cyclonic activity over northern Europe and by stronger-than-normal Greenland High – both triggering the northeastern airflow to the Northern Atlantic. Weakening Greenland High in the negative phase of PC1 and anticyclonic conditions over northern Scandinavia and Russia cause the reverse, namely, southwestern inflow, which brings warm air to the central part of the Atlantic Arctic. PC1 is the only circulation pattern, that modifies air temperature over the Svalbard Archipelago, where the correlation coefficient is $<–0.5$, or even $<–0.6$ on the southwestern edge of the Spitsbergen Island.

A much lower impact on the air temperature is noted under the PC2 type, and |r| values hardly exceed 0.2. The negative relationship is a little stronger ($r<–0.3$) only over Iceland, where, in a western sector of a deep cyclone, forming in the Norwegian Sea region in a positive PC2 phase, northern circulation prevails over Spitsbergen. The third most important circulation type PC3 strongly modifies air temperature in the eastern and western parts of the studied area. Anticyclonic conditions in the center of the Atlantic Arctic under the positive phase of PC3 trigger the northeastern circulation in the eastern part of the study area, and the southeastern inflow over Greenland. In the PC3 negative phase, counter clockwise circulation around the cyclone located over Spitsbergen activates southern/northern airflow in the east/west of the studied area, causing an increase in winter air temperature in the Barents Sea region and a decrease over Greenland. The remaining circulation types (PC4–PC6), explaining only 5–8% of the total variance of the SLP field each, do not significantly modify the air temperature at 850 hPa geopotential level over the Atlantic Arctic. The correlation coefficient exceeds |0.4| only under the PC6 in southwestern Greenland.
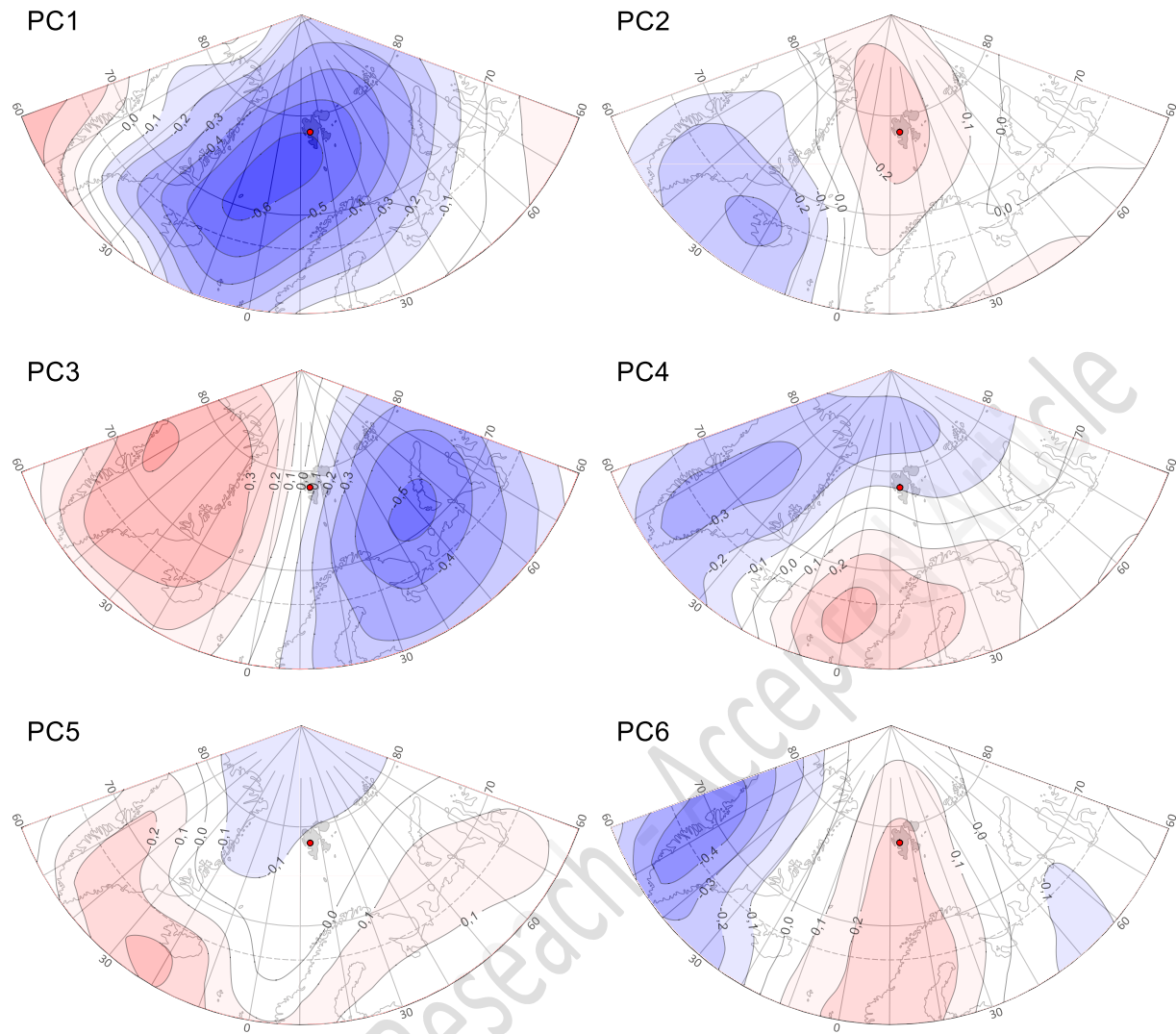
Fig. 9. Correlation between daily indices of PC1–PC6 circulation patterns and daily air temperature anomalies at 850 geopotential level in winter (Dec–Mar), based on data from the period 1976–2021. Svalbard Archipelago is shaded grey; Svalbard Lufthavn station is marked with a red dot.

The correlation fields in Fig. 9 display significant values over the Svalbard Archipelago only in the case of PC1, which means that only the first circulation type modifies the low-tropospheric temperature in this area. It was also affirmed for the surface air temperature, as the correlation coefficient between PC's daily indices and the daily mean air temperature anomalies in the Svalbard Lufthavn station is the highest (–0.55) and statistically significant only for PC1 (Table 3). It is not surprising, as the PC1 type reflects exactly the pattern of the correlation field between the winter anomalies of daily mean surface air temperature in the Svalbard Lufthavn station and the grid-points SLP values shown in Fig. 6 (DJFM). The extended zonally bipolar pattern of both the DJFM correlation field and PC1 indicates northern/southern airflow over

Spitsbergen, causing a substantial decrease/increase in air temperature. The other five detected circulation patterns do not significantly modify the air temperature in the Svalbard Lufthavn station and the absolute values of correlation coefficients between temperature anomalies and circulation indices do not exceed 0.2.

Finally, an attempt was made to find the trends of changes in the phase and intensity of each circulation type. While there is a distinct winter-to-winter variability in the intensity of each circulation pattern, not any trends in the mean Dec–Mar indices, nor particularly significant periods of positive or negative phases were detected in the period 1976–2021 (Fig. 10). This may suggest, that the regional-scale circulation patterns, although distinctly modify the temperature field in winter and impact its low-frequency changes, neither intensify nor suppress the progressive warming in the Atlantic Arctic.
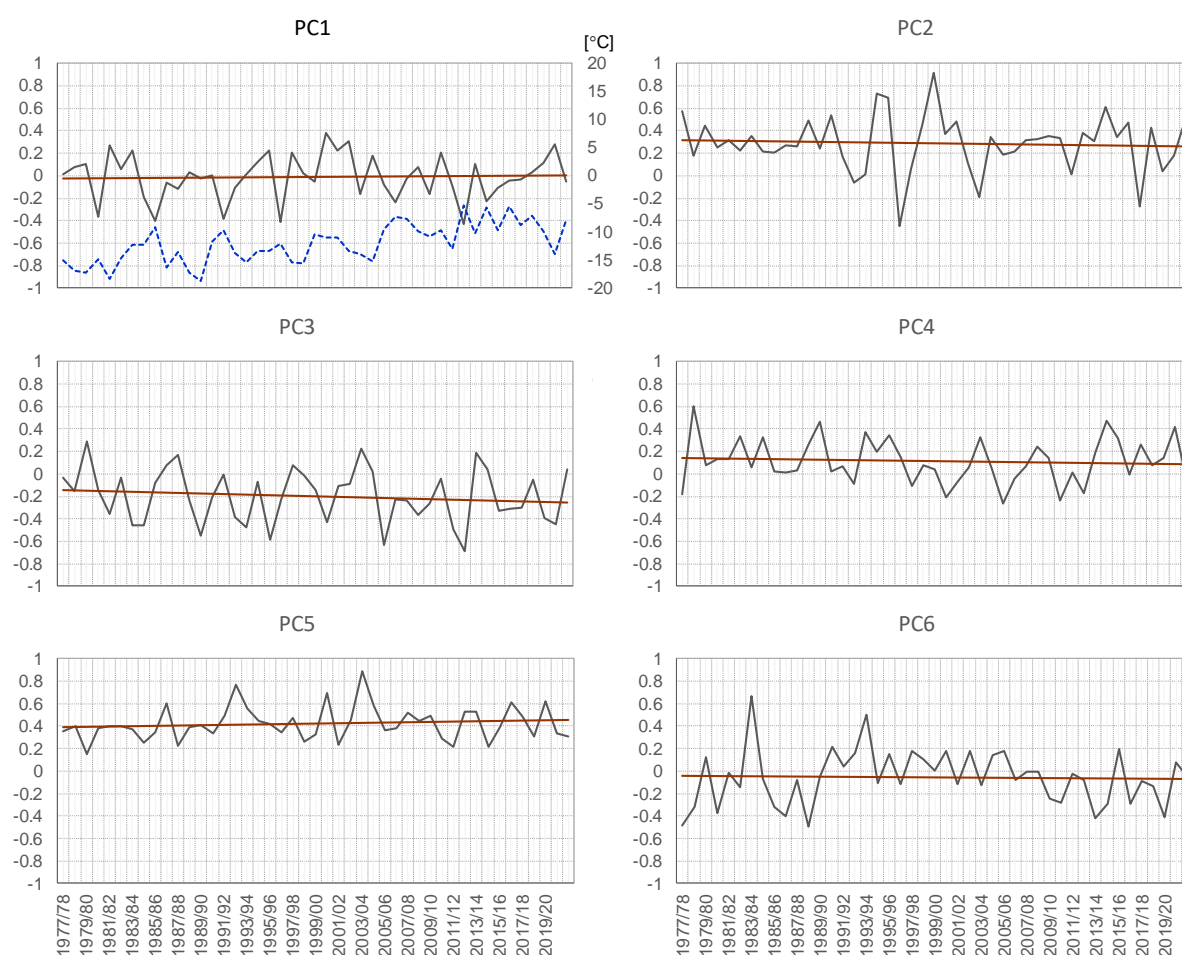

Fig. 10. Multiannual course of mean winter (Dec–Mar) indices of PC1−PC6 circulation patterns with a trend line (red) and winter air temperature variability (°C) in Svalbard Lufthavn station (blue dashed line) added to PC1

Discussion

The study confirmed an increase in mean annual and mean seasonal air temperature in winter. More intensive changes were determined in the case of seasonal fluctuations, reaching 1.83°C per decade for the analysed period 1976/77–2020/21. As the Arctic warming accelerated during the first two decades of the 21st century (Chylek *et al.* 2022), the warming rate for the Svalbard Lufthavn station computed for a more recent period would be higher. Less intense winter warming computed for the same period (1976/77–2020/21) occurred in the low troposphere and it did not exceed 0.8°C per decade. The lower-tropospheric warming structure with the rate of changes decreasing upwards is connected with a decrease in sea ice extent (particularly important in the melt season) and surface-amplified warming, weakened boundary layer temperature inversions, connected with reducing net longwave cooling at the surface (Kaufman and Feldl 2022).

The obtained results are in accordance with earlier research that has shown variable trends in air temperature in a year, and intensive warming in the winter season (Bednorz 2011; Isaksen *et al.* 2016; Johannessen *et al.* 2016; Tomczyk *et al.* 2019; Łupikasza *et al.* 2021). Particularly warm years and winters were recorded at the beginning of the 21st century. According to long-term study results, the recent years have been the warmest years in more than a century of instrumental observations (Nordli *et al.* 2014; Gjelten *et al.* 2016; Łupikasza and Niedźwiedź 2019; Hanssen-Bauer *et al.* 2019).

The consequence of the progressing warming was the increasingly frequent occurrence of warm days, and the increasingly seldom occurrence of cold days. The study showed more intensive changes in the case of cold days, which occurred only in season 2019/20 over the recent decade. More seldom occurrence of single days, but also sequences of several days have been observed in recent decades. According to Tomczyk *et al.* (2019), cold waves in summer occurred increasingly seldom, and warm waves occurred increasingly frequently in winter. The recorded changes were more intensive in the central than in north-western Spitsbergen. The currently observed warming is more intensive than the warming from the beginning of the 20th century. According to Przybylak *et al.* (2022), days with maximum air temperature below 0°C were more frequently recorded during the ETCAW warming than currently, and the frequency of days with maximum air temperature exceeding 0°C shows the opposite trend.

Surface weather conditions and their day-to-day variability, as well as the occurrence of the meteorological extremes in the Spitsbergen area, are strongly influenced by air circulation

(Kejna and Sobota 2019; Araźny *et al.* 2022). The air temperature, both at the surface and in the low troposphere is particularly sensitive to short-term changes in regional-scale circulation. Przybylak *et al.* (2018) observed the greatest variability of thermal parameters in NW Spitsbergen during air advection from the eastern sector, particularly pronounced in the cold season.

The PCA method was applied to SLP data to recognize daily circulation patterns. Although PCA is recognized as the best method for circulation classification purposes, it still has some shortcomings, for example, the dependence of outputs of PCA on the shape and size of the domain on which the analysis is conducted, particularly if unrotated, thus the association of the outputs of PCA with physical processes is not always straightforward (Huth 1996; Huth and Beranova 2020; Spensberger *et al.* 2020).

Among the six regional circulation patterns recognized in the daily timescale at the sea level by the means of PCA, the pattern representing the first PC appeared to have the strongest impact on the low-tropospheric temperature variability in the Svalbard area. The position of the centers of action in this dominating pattern strongly resembles the Barents Oscillation recognized by Skeie (2000) and Chen *et al.* (2013) as the second EOF of monthly SLP anomalies poleward of 30°N with a primary center of action over the Barents Region, and another center of the opposite sign located over Greenland. PC1 strongly influences the air temperature in the low troposphere in winter (Dec–Mar) over the Greenland Sea (r>0.6) and is the only regional circulation pattern that modifies low-frequency temperature variability at Svalbard Lufthavn station.

The second after PC1 circulation pattern having a strong impact on the temperature field in the Atlantic Arctic is PC3. In winter, it rather tends to be in the negative phase, which expresses the low pressure centered over Svalbard, and to rise temperature over the Barents Sea (correlation <–0.5). The PC1 pattern resembles the 'European Blocking' pattern identified by Champagne *et al.* (2019), who recognized variability patterns of the Atlantic-Arctic region atmosphere in the area 80°W to 90°E longitude and 50°N to 90°N latitude, at 500 hPa geopotential height 500 hPa, using the k-means method. The Barents Sea 'center of action' was also recognized by Rogers *et al.* (2005) as exhibiting intensive cyclogenesis in winter, earlier identified by Serreze and Barry (1988) and Serreze *et al.* (1993).

The PC2 pattern is similar to the 'Atlantic Through' in Champagne *et al.* (2019), while PC4 and PC6 indicate the Icelandic Low and Fram Strait 'centers of action' described by Rogers *et al.* (2005). Cyclones occurring in the Fram Strait (like in the PC6 positive phase) are associated with positive winter temperature extremes in Spitsbergen (Bednorz 2011).

The results obtained in this study demonstrate that the high day-to-day variability in the winter air temperature in the Atlantic region of the Arctic is strongly controlled by the regional pressure systems and the advection of air masses. On the other hand, the multiannual trends in low-tropospheric temperature strongly manifested in the Arctic are not associated with trends in the intensity of circulation patterns recognized by the PCA in the Atlantic Arctic region. This confirms the results obtained by Isaksen *et al.* (2016) who claim that changes in frequencies of atmospheric circulation types play a minor role in the total recent surface warming. They claim, that the strong warming in Spitsbergen in the latest decades is not driven by increased frequencies of "warm" atmospheric circulation types but rather from sea ice decline, higher sea surface temperatures, and a general background warming.

Conclusions

Significant increasing trends in the low-tropospheric air temperature over the Atlantic Arctic in the years 1976–2021 were confirmed in the study. The temperature increase is faster in the winter months, both in the Svalbard Lufthavn meteorological station and in the entire low-tropospheric temperature field in the Svalbard region. The winter months are also characterized by a higher variability, although, the number of positive temperature extremes has been growing during the analysed 45 winter seasons, while negative extremes appeared very rarely in the last decade of the study period. The variability in winter temperature can be explained by the low-frequency variability in regional-scale circulation patterns. Six daily circulation patterns, explaining 76.3% daily variability in the SLP field were recognized in the studied area. Some of them strongly modify the air temperature in the region, particularly the most relevant bipolar pattern, resembling the Barents Oscillation, with centers located over Greenland and the White Sea. The determined circulation patterns influence the low-frequency temperature variability, however, they play a minor role in the total recent surface warming trends.

References

Alekseev G., Glok N. and Smirnov A. 2016. On assessment of the relationship between changes of sea ice extent and climate in the Arctic. *International Journal of Climatology* 36: 3407–3412. doi: 10.1002/joc.4550

AMAP 2021. *AMAP Arctic Climate Change Update 2021: Key Trends and Impacts*. Arctic Monitoring and Assessment Programme (AMAP), Tromsø, Norway.

Araźny A., Przybylak R. and Kejna M. 2022. The influence of atmospheric circulation on mean and extreme weather conditions on Kaffiøyra (NW Spitsbergen, Svalbard Archipelago) in the Summer Seasons 1975–2015. *Frontiers in Environmental Science* 10: 1–14. doi: 10.3389/fenvs.2022.867106

Barnston A. and Livezey R. 1987. Classification, seasonality and persistence of low-frequency atmospheric circulation patterns. *Monthly Weather Review* 115: 1083–1126. doi: 10.1175/1520-0493(1987)115<1083:CSAPOL>2.0.CO;2

Bednorz E. 2011. Occurrence of winter air temperature extremes in Central Spitsbergen. *Theoretical and Applied Climatology* 106: 547–556. doi: 10.1007/s00704-011-0423-y

Bengtsson L., Semenov V.A. and Johannessen O.M. 2004. The early twentieth-century warming in the Arctic—A possible mechanism. *Journal of Climate* 17: 4045–4057. doi: 10.1175/JCLI-D-15-0042.1

Cai L., Alexeev V.A., Walsh J.E. and Bhatt U.S. 2018. Patterns, impacts, and future projections of summer variability in the Arctic from CMIP5 models. *Journal of Climate* 31: 9815–9833. doi: 10.1175/JCLI-D-18-0119.1

Champagne O., Pohl B., McKenzie S., Buoncristiani J.F., Bernard E., Joly D. and Tolle F. 2019. Atmospheric circulation modulates the spatial variability of temperature in the Atlantic–Arctic region. *International Journal of Climatology* 39: 3619–3638. doi: 10.1002/joc.6044

Chen H.W., Zhang Q., Körnich H. and Chen D. 2013. A robust mode of climate variability in the Arctic: The Barents Oscillation. *Geophysical Research Letters* 40: 2856–2861. doi: 10.1002/grl.50551

Chylek P., Folland C., Klett J. ., Wang M., Hengartner N., Lesins G. and Dubey M.K. 2022. Annual mean arctic amplification 1970–2020: observed and simulated by CMIP6 climate models. *Geophysical Research Letters* 49: e2022GL099371. doi: 10.1029/2022GL099371

Deser C. 2000. On the teleconnectivity of the "Arctic Oscillation". *Geophysical Research Letters* 27: 779–782. doi: 10.1029/1999GL010945

Esteban P, Jones P, Martín-Vide J. and Mases M. 2005. Atmospheric circulation patterns related to heavy snowfall days in Andorra, Pyrenees. *International Journal of Climatology* 25: 319–329. doi: 10.1002/joc.1103

Fang Z-F. 2004. Statistical relationship between the northern hemisphere sea ice and atmospheric circulation during winter time. *In*: Zhu X (ed.) *Observation, Theory and Modeling of Atmospheric Variability.* World Scientific Series on Meteorology of East Asia, World Scientific Publishing Company, Singapore: 131–141.

Fyfe J.C., von Salzen K., Gillett N.P., Arora V.K., Flato G.M. and McConnell J.R. 2013. One hundred years of Arctic surface temperature variation due to anthropogenic influence. *Scientific Reports* 3: 2645. doi: 10.1038/srep02645

Gjelten H.M., Nordli Ø., Isaksen K., Førland E., Sviashchennikov P., Wyszyński P., Prokhorova U., Przybylak R., Ivanov B. and Urazgildeeva A. 2016. Air temperature variations and gradients along the coast and fjords of western Spitsbergen. *Polar Research* 35: 29878. doi: 10.3402/polar.v35.29878

Hanna E., Cropper T.E., Hall R. J. and Cappelen J. 2016. Greenland Blocking Index 1851–2015: a regional climate change signal. *International Journal of Climatology* 36: 4847–4861. doi: 10.1002/joc.4673

Hanssen-Bauer I., Førland Ej, Hisdal H., Mayer S., Sandø A.B. and Sorteberg A. 2019. *Climate in Svalbard 2100 - a knowledge base for climate adaptation*. Norway, Norwegian Centre of Climate Services (NCCS) for Norwegian Environment Agency (Miljødirektoratet). doi: 10.25607/OBP-888

Huth R. 1996. Properties of the circulation classification scheme based on the rotated principal component analysis. *Meteorology and Atmospheric Physics* 59: 217–233. doi: 10.1007/BF01030145

Huth R. and Beranová R. 2021. How to recognize a true mode of atmospheric circulation variability. *Earth and Space Science* 8:e2020EA001275. doi: 10.1029/2020EA001275

Huth R., Beck C., Philipp A., Demuzere M., Ustrnul Z., Cahynová M., Kyselý J. and Tveito O.E. 2008. Classifications of atmospheric circulation patterns: recent advances and applications. *Annals of the New York Academy of Sciences* 1146: 105–152. doi: 10.1196/annals.1446.019

Isaksen K., Nordli O., Forland E.J., Łupikasza E., Eastwood S. and Niedźwiedz T. 2016. Recent warming on Spitsbergen - influence of atmospheric circulation and sea ice cover. *Journal of Geophysical Research: Atmospheres* 121: 11.913–11.931. doi: 10.1002/2016JD025606

Johannessen O., Kuzmina S., Bobylev L. and Miles M. 2016. Surface air temperature variability and trends in the Arctic: New amplification assessment and regionalisation. *Tellus A: Dynamic Meteorology and Oceanography* 68: 28234. doi: 10.3402/tellusa.v68.28234

Johannessen O.M., Bengtsson L., Miles M.W., Kuzmina S.I., Semenov V.A. and Alekseev G.V., et al. 2004. Artic climate change: observed and modelled temperature and sea ice variability. *Tellus A: Dynamic Meteorology and Oceanography* 56: 328–341. doi: 10.3402/tellusa.v56i4.14418

Kalnay E., Kanamitsu M., Kistler R., Collins W., Deaven D., Gandin L., Iredell M., Saha S., White G., Woollen J., Zhu Y., Leetmaa A., Reynolds R., Chelliah M., Ebisuzaki W., Higgins W., Janowiak J., Mo K., Ropelewski C., Wang J., Jenne R. and Joseph D. 1996. The NCEP/NCAR 40-year reanalysis project. *Bulletin of the American Meteorological Society* 77: 437–471. doi: 10.1175/1520-0477(1996)077<0437:TNYRP>2.0.CO;2

Kaufman Z.S. and Feldl N. 2022. Causes of the Arctic's Lower-Tropospheric Warming Structure. *Journal of Climate* 35: 1983–2002. doi: 10.1175/JCLI-D-21-0298.1

Kejna M. and Sobota I. 2019. Meteorological conditions on Kaffiøyra (NW Spitsbergen) in 2013–2017 and their connection with atmospheric circulation and sea ice extent. *Polish Polar Research* 40: 175–204. doi: 10.24425/ppr.2019.129670

Kendall M. 1975. *Multivariate Analysis*. Charles Griffin & Company, London.

Łupikasza E. and Niedźwiedź T. 2013. Frequency of ice days at selected meteorological stations in Svalbard. *Bulletin of Geography – Physical Geography Series* 6/2013: 80–97. doi: 10.2478/bgeo-2013-0005

Łupikasza E.B. and Niedźwiedź T. 2019. The influence of mesoscale atmospheric circulation on Spitsbergen air temperature in periods of Arctic warming and cooling. *Journal of Geophysical Research: Atmospheres* 124: 5233–5250. doi: 10.1029/2018JD029443

Łupikasza E.B., Niedźwiedź T., Przybylak R. and Nordli O. 2021. Importance of regional indices of atmospheric circulation for periods of warming and cooling in Svalbard during 1920–2018. *International Journal of Climatology* 41: 3481–3502. doi: 10.1002/joc.7031

Mann H.B. 1945. Nonparametric tests against trend. *Econometrica: Journal of the Econometric Society* 13: 245–259.

Matthes H., Rinke A. and Dethloff K. 2015. Recent changes in Arctic temperature extremes: warm and cold spells during winter and summer. *Environmental Research Letters* 10: 029501. doi: 10.1088/1748-9326/10/11/114020

NCAR (National Center for Atmospheric Research) Staff (eds.). 2015. The Climate Data Guide: Overview: Climate Indices. Retrieved from https://climatedataguide.ucar.edu/climate-data/overviewclimate-indices.

Niedźwiedź T., Łupikasza E. and Małarzewski Ł. 2012. The influence of atmospheric circulation on the occurrence of frosty days in Hornsund (Spitsbergen). *Problemy Klimatologii Polarnej* 22: 17–26 (in Polish).

Nordli Ø. 1990. Temperature and precipitation series at Norwegian Arctic meteorological stations. DNMI KLIMA. *Raport* 40: 1–14.

Nordli Ø., Przybylak R., Ogilvie A.E. and Isaksen K. 2014. Long-term temperature trends and variability on Spitsbergen: the extended Svalbard Airport temperature series, 1898–2012. *Polar Research* 33: 21349. doi: 10.3402/polar.v33.21349

Nozawa T., Nagashima T., Shiogama H. and Crooks S.A. 2005. Detecting natural influence on surface air temperature change in the early twentieth century. *Geophysical Research Letters* 32: L20719. doi: 10.1029/2005GL023540

Overland J.E. and Wang M. 2010. Large-scale atmospheric circulation changes are associated with the recent loss of Arctic sea ice. *Tellus A: Dynamic Meteorology and Oceanography* 62: 1–9. doi: 10.1111/j.1600-0870.2009.00421.x

Overland J.E., Wood K. and Wang M. 2011. Warm Arctic - cold continents: climate impacts of the newly open Arctic Sea. *Polar Research* 30: 15787. doi: 10.3402/polar.v30i0.15787

Park D.-S.R., Lee S. and Feldstein S.B. 2015. Attribution of the recent winter sea ice decline over the Atlantic sector of the Arctic Ocean. *Journal of Climate* 28: 4027–4033. doi: 10.1175/JCLI-D-15-0042.1

Polyakov I.V., Timokhov L.A., Alexeev V.A., Bacon S., Dmitrenko I.A., Fortier L., Frolov I.E., Gascard J.-C., Hansen E., Ivanov V.V., Laxon S., Mauritzen C., Perovich D., Shimada K., Simmons H.L., Sokolov V.T., Steele M. and Toole J. 2010. Arctic Ocean warming contributes to reduced polar ice cap. *Journal of Physical Oceanography* 40: 2743–2756. doi: 10.1175/2010JPO4339.1

Przybylak R. 2016. *The Climate of the Arctic*. Second Edition. *Atmospheric and Oceanographic Sciences Library* 52: 1–287.

Przybylak R. and Wyszyński P. 2020. Air temperature changes in the Arctic in the period 1951–2015 in the light of observational and reanalysis data. *Theoretical and Applied Climatology* 139: 75–94. doi: 10.1007/s00704-019-02952-3

Przybylak R., Araźny A. and Ulandowska-Monarcha P. 2018. The influence of atmospheric circulation on the spatial diversity of air temperature in the area of Forlandsundet (NW Spitsbergen) during 2010–2013. *International Journal of Climatology* 38: 230–251. doi: 10.1002/joc.5172

Przybylak R., Wyszyński P. and Araźny A. 2022. Comparison of early-twentieth-century Arctic warming and contemporary arctic warming in the light of daily and subdaily data. *Journal of Climate* 35: 2269–2290. doi: 10.1175/JCLI-D-21-0162.1

Rogers J.C., Yang L. and Li L. 2005. The role of Fram Strait winter cyclones on sea ice flux and on Spitsbergen air temperatures. *Geophysical Research Letters* 32: L06709. doi: 10.1029/2004GL022262

Salmi T., Maiittii A., Anttila P., Ruoho-Airola T. and Amnel T. 2002. Detecting trends of annual values of atmospheric pollutants by the Mann-Kendall test and Sen's slope estimates - the Excel template application MAKESENS. *Finnish Meteorological Institute, Public On Air Quality* 31: 1–35.

Serreze M.C. and Barry R.G. 1988. Synoptic activity in the Arctic Basin 1979–85. *Journal of Climate* 1: 1276–1295. doi: 10.1175/1520-0442(1988)001<1276:SAITAB>2.0.CO;2

Serreze M.C. and Francis J.A. 2006. The Arctic amplification debate. *Climatic Change* 76: 241–264. doi: 10.1007/s10584-005-9017-y

Serreze M.C., Box R.G., Barry R.G. and Walsh J.E. 1993. Characteristics of Arctic synoptic activity. *Meteorology and Atmospheric Physics* 51: 147–164.

Severe Weather Europe. 2020. https://www.severe-weather.eu/news/svalbard-record-heat-norway-mk/.

Skeie P. 2000. Meridional flow variability over the Nordic seas in the Arctic Oscillation framework. *Geophysical Research Letters* 27: 2569–2572. doi: 10.1029/2000GL011529

Spensberger C., Reeder M.J., Spengler T. and Patterson M. 2020. The connection between the Southern Annular Mode and a feature-based perspective on Southern Hemisphere midlatitude winter variability. *Journal of Climate* 33: 115–129. doi: 10.1175/JCLI-D-19-9224.1

Thompson D.W. and Wallace J.M. 1998. The Arctic Oscillation signature in the wintertime geopotential height and temperature fields. *Geophysical Research Letters* 25: 1297–1300. doi: 10.1029/98GL00950

Tokinaga H., Xie S.P., and Mukougawa H. 2017. Early 20th century Arctic warming intensified by Pacific and Atlantic multidecadal variability. *Proceedings of the National Academy of Sciences* 114: 6227–6232. doi: 10.1073/pnas.161588011

Tomczyk A.M. and Bednorz E., 2014. Warm waves in north–western Spitsbergen. *Polish Polar Research* 35: 497–511. doi: 10.1007/s00704-012-0798-4

Tomczyk A.M., Łupikasza E.B. and Kendzierski S. 2019. Warm winter and cold summer spells in Spitsbergen and their circulation conditions. *Polish Polar Research* 40: 339–359. doi: 10.24425/ppr.2019.130902

Vikhamar-Schuler D., Isaksen K., Haugen J.E., Tømmervik H., Luks B., Schuler T.V. and Bjerke J.W. 2016. Changes in winter warming events in the Nordic Arctic Region. *Journal of Climate* 29: 6223–6244. doi: 10.1175/JCLI-D-15-0763.1

Wang D., Wang C., Yang X. and Lu J. 2005. Winter Northern Hemisphere surface air temperature variability associated with the Arctic Oscillation and North Atlantic Oscillation. *Geophysical Research Letters* 32: L16706. doi: 10.1029/2005GL022952

Wei T., Ding M., Wu B., Lu C. and Wang S. 2016. Variations in temperature-related extreme events (1975–2014) in Ny-Ålesund, Svalbard. *Atmospheric Science Letters* 17: 102–108. doi: 10.1002/asl.632

Wilks D. 2011. *Statistical methods in the atmospheric sciences*. Elsevier Academic Press, Amsterdam

WMO 2020. https://www.climatecentre.org/7397/wmo-verifies-mediterranean-temperature-that-set-new-arctic-record/

Yarnal B. 1993. *Synoptic climatology in environmental analysis*. Belhaven, London